Journal of
Materials Chemistry A

Accepted Manuscript

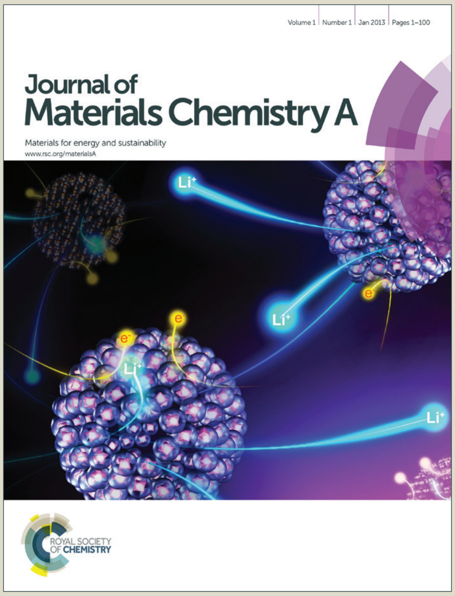

ROYAL SOCIETY
OF **CHEMISTRY**

www.rsc.org/materialsA

Performance enhancement of quantum dot sensitized solar cells by adding electrolyte additives

Jun Du, Xinxin Meng, Ke Zhao, Yan Li* and Xinhua Zhong*

Key Laboratory for Advanced Materials, Institute of Applied Chemistry, East China University of Science and Technology, Shanghai 200237, China

Email: yli@ecust.edu.cn (for Y. L.); zhongxh@ecust.edu.cn (for X. Z.)

Tel/Fax: (+86) 21 6425 0281

Abstract

Besides relatively high redox potential of the adopted S^{2-}/S_n^{2-} polysulfide redox couple electrolyte, the parasitic charge recombination processes is another significant factor that limits the open-circuit voltage and consequent power conversion efficiency (PCE) of quantum dot sensitized solar cells (QDSCs). Herein, we report a facile method to modify the polysulfide electrolyte with addition of polyethylene glycol (PEG) additives to suppress the charge recombination occurring at the TiO_2/QDs/electrolyte interfaces. Impedance spectroscopy and open circuit voltage decay (OCVD) measurements reveal that the PEG additive in polysulfide electrolyte reduces interfacial recombination when compared with conventional polysulfide electrolyte in the absence of PEG additive. A dramatic enhancement of PCE from 5.80% to 6.74% was observed with the introduction of 15 wt% PEG in the polysulfide electrolyte in CdSe based QDSCs. Moreover, the PEG additive also improves the photovoltaic performance stability of the resultant cells.

1. Introduction

Due to the unique optoelectronic properties, such as high light absorption coefficient, conveniently tunable light harvesting range, and large dipole etc., the application of semiconductor quantum dots (QDs) as alternative light harvesting material to conventional molecular dyes in sensitized solar cells are attracting increasing attention.[1–5] Similar to its analogue dye sensitized solar cells (DSCs), quantum dot sensitized solar cells (QDSCs) comprise a photoanode (QD-sensitized mesoporous nanocrystalline metal oxide, commonly TiO_2), counter electrode, and electrolyte.[6–8] As a vital component of QDSCs, electrolyte preforms the function of QD regeneration as well as the charge transfer between the photoanode and counter electrode.[9,10] Polysulfide (S^{2-}/S_n^{2-}) redox couple aqueous solution electrolyte is commonly used in QDSCs since this electrolyte media can stabilize the commonly used chalcogenide QD sensitizers and can also offer an acceptable photovoltaic performance of the resultant QDSCs.[11–15] Because of the relatively high redox potential of polysulfide electrolyte, the obtained open-circuit (V_{oc}) values in QDSCs, usually less than 0.65 V, are substantially lower than those in DSCs (up to 1.0 eV).[16–20] To improve the photovoltaic performance especially the V_{oc} value in QDSCs, alternative redox couples with a relatively low redox potential, including I^-/I_3^-,[21] $Co^{2+/3+}$ complex,[22,23] and organic redox couple[24–26] have been explored. Unfortunately, the commonly used cadmium chalcogenide QDs can hardly survive in the above mentioned electrolyte media, with a poor stability of the resultant cell devices.

Besides the redox potential of electrolyte system, the parasitic charge recombination processes is another important factor that affects V_{oc} and the consequent power conversion efficiency (PCE) of cell devices.[27] A known method to improve the photovoltaic performance in DSC system is the introduction of series of additives such as deoxycholic acid (DCA),[28] 4-tert-butylpyridine (TBP)[29] and guanidinium thiocyanate (GuSCN),[30] into the I^-/I_3^- electrolyte. These additives can suppress the charge recombination and tune Fermi level of TiO_2, therefore brings forward the improvement of performance in the resulting DSC devices. These empirical success promotes us to modify the polysulfide electrolyte with electrolyte additives to improve the performance of the resulting QDSCs. In fact, similar work has been explored in recent reports on QDSCs.[31–38] For example, polysulfide based hydrogel or ionic liquid electrolyte was tested in QDSCs to improve the stability of the designed cells.[31–36] Molecular dipoles were used to tune the Fermi level of TiO_2 and therefore affect the V_{oc}.[37,38] Although recent advances are very impressive, the improvement of the cell stability is at the scarification of photovoltaic performance or *vice versa* in almost all of the previous literatures. Therefore, the further development of QDSCs with both high PCE and long-term stability is highly desirable, and also becomes a great challenge.

Herein, we report a modified polysulfide electrolyte with addition of polyethylene glycol (PEG) to increase the performance (including both PCE and cell stability) of the resultant QDSCs. As a kind of nonionic polymer, PEG was commonly used as a stabilizer or a capping ligand in the preparation of inorganic nanomaterials because it could adsorb onto the surface of nanoparticles *via* the strong interaction force.[39,40] It is expected that the PEG additives in polysulfide electrolyte can serve as a protective layer over both TiO_2 and QDs surfaces by the steric hindrance effect, consequently retarding the unwanted charge recombination between the photoanode and the electrolyte and improving the photovoltaic performance of QDSCs. CdSe based QDSCs were selected as a model cell to evaluate the effect of the modified redox electrolyte. Experimental results indicate that the PCE of QDSCs based on polysulfide electrolyte containing optimal concentration of PEG show an improvement of 16.2% over the reference cells using polysulfide electrolyte without PEG additive, together with an additional beneficial effect of improved cell stability.

2. Experimental section

Chemicals

Oleic acid (90%) and 3-mercaptopropionic acid (MPA, 98%) were purchased from Alfa Aesar. 1-octadecene (ODE, 90%), selenium powder (200 mesh, 99.99%), trioctylphosphine (TOP, 90%), cadmium oxide (CdO, 99.99%), oleylamine (OAm, 95%), sulfur powder (99.99%), polyethylene glycol (PEG) (20000) and PEG (4000) were received from Aldrich. All reagents were used as received without any further purification.

Preparation of Oil-soluble CdSe QDs

The oil-soluble CdSe QDs capped by oleylamine (OAm) were synthesized by a minor modified literature method.[41] Typically, 0.4 mL of 1.0 M Se solution prepared by dissolving Se powder into trioctylphosphine (TOP) was mixed with 0.6 mL of TOP and 10 mL of OAm. Under the protection of high purity nitrogen, the above solution was heated to 275 ^{o}C, followed by the injection of 1.0 mL of 0.4 M Cd precursor prepared by dissolving CdO in oleic acid and ODE (v/v, 1:1) at 250 ^{o}C. Then, the reaction system was heated to 285 ^{o}C and kept at this temperature for 6 min. After precipitation and centrifugation procedure with the addition of methanol and acetone, the purified oil-soluble CdSe QDs with average particle size of 5.4 ± 0.4 nm was obtained. The oil-soluble CdSe QDs was dispersed in chloroform solution for further use. The transmission electronic microscopy (TEM) images, PL emission and absorption spectra of the obtained CdSe QDs are available in Fig. S1 of the ESI.† The absorption spectra of the CdSe QDs films with and without PEG-polysulfide electrolyte treatment have also been given in Fig S2 in ESI.†

Preparation of MPA-capped water-soluble CdSe QDs

The hydrophilic CdSe QDs were prepared according to our reported procedure.[42,43] Briefly, 2 mmol of MPA was dissolved in 1.0 mL methanol, and the pH value was then adjusted to 10.0 by the addition of NaOH aqueous solution. The above MPA-methanol solution was added into 20 mL of CdSe QD chloroform solution with stirring at room temperature for 120 min.

The MPA capped CdSe QDs were extracted from chloroform solution by adding 20.0 mL deionized water. After centrifugation and precipitation, the hydrophilic CdSe QDs capped by MPA were obtained. The obtained MPA capped CdSe QDs was dispersed in 1.5 mL deionized water followed by adjusting pH value to 10 for further use.

Assembly of the sealed QDSCs

According to the reported method, the TiO_2 mesoporous film electrodes composed of transparent layer (9.0 ± 0.5 μm) and light scattering layer (6.0 ± 0.5 μm) was first prepared through the screen-printing technique over the FTO glass substrate (8 Ω/square) that was pre-treated by $TiCl_4$ aqueous solution (0.04 M).[44] During cell device construction, the sensitized photoanode were obtained by pipetting MPA-capped water-soluble CdSe QDs on TiO_2 film electrodes and staying for 2 h. According to our previous study,[45] the inorganic ZnS/SiO_2 overcoating layers can form the energy barriers over the surface of the photoanode, and accordingly suppress the unwanted charge recombination between the photoanode and the electrolyte. Therefore, the adopted photoanodes were then treated with ZnS/SiO_2 double barrier coating layers. Typically, the CdSe QD-sensitized TiO_2 film electrodes were first coated with ZnS barrier layer by dipping the electrode alternately into 0.1 M $Zn(OAc)_2$ solution in methanol and 0.1 M Na_2S solution in methanol and water mixture solvent (1/1, v/v) for 4 cycle with 1 min/dip, followed by sintering at 300 ^oC for 2 min. After cooling to room temperature, the photoanodes were soaked in a tetraethoxysilane (TEOS) solution (containing of TEOS, ammonium hydroxide, 2:8 (v/v) mixture of deionized water and ethanol) at 35 ^oC for 2 h to form a SiO_2 layer on the surface of QDs and TiO_2.[45]

The cell was assembled by agglutinating the CdSe-sensitized TiO_2 photoanodes and the $Cu_{2-x}S$/FTO CE using a Surlyn ring (DuPont) of 60 μm thickness. The electrolyte was injected into the cells *via* pre-drilled holes on the counter electrode, and the hole was then sealed with a thin glass slide. A black mask (0.125 cm^2) was used in the subsequent photovoltaic studies. All cell samples studied were constructed with the same batch of photoanodes and $Cu_{2-x}S$/FTO counter electrodes but with polysulfide electrolytes (1.0 M Na_2S and S aqueous solution) containing different concentrations of PEG. To minimize the sampling deviation, the average photovoltaic performances of five cell devices in parallel under each electrolyte composition were adopted. $Cu_{2-x}S$/FTO counter electrode were prepared according to literature method by screen-printing pre-prepared $Cu_{2-x}S$ nanoparticles on FTO substrate.[46] Detailed procedures are described in the ESI.†

Characterization

The UV/vis absorption and photoluminescence (PL) emission spectra were conducted using a UV-visible spectrophotometer (Shimadzu UV-3101 PC) and a fluorescence spectrophotometer (Cary Eclipse Varian), respectively. Transition electron microscopy (TEM) images were obtained on a JEOL JEM-2100 microscope with accelerating voltage of 200 kV. The samples for TEM were prepared by dropping dilute QD dispersion in toluene on copper grids with a carbon support followed by drying naturally in air at room temperature. Current-voltage curves (*J–V* curves) of the cell devices were tested using a Keithley 2400 source meter under illumination of simulated AM 1.5G solar light (Oriel, Model No.94022A) with an intensity of 100 mW cm^{-2} (1 full sun). Photoactive area was 0.235 cm^2 defined by a black plastic disk, while a black mask with an aperture area of 0.125 cm^2 was used during measurement to avoid stray light completely. Incident photon-to-current conversion efficiency (IPCE) spectrum was measured using a Keithley 2000 multimeter, and a spectral product DK240 monochrometer with 300W tungsten lamp provided illumination. Electrochemical impedance spectroscopy (EIS) and open circuit voltage decay (OCVD) measurements were carried out on an electrochemical workstation (Zahner, Zennium). EIS was measured under dark conditions at different forward bias ranged from 0 V to 0.60 V, applying a 20 mV AC sinusoidal signal over the constant applied bias with the frequency ranging from 1 MHz to 0.1 Hz. In OCVD measurements, samples were illuminated by a white LED with intensity of 100 mW cm^{-2}, and the dependence of photovoltage on time was recorded after switch-off of the light.

3. Results and discussion

To evaluate the effect of PEG additive in polysulfide electrolyte and determine the optimum concentration of PEG used, a model CdSe QDSC was constructed by our recently developed capping ligand induced self-assembly approach.[42,43,47] Due to the convenient availability and effectiveness, PEG-4000 and PEG-20000 were the most used PEG series product in previous literatures.[48] Herein, a mixture of PEG-4000 and PEG-20000 with weight ratio of 1:1 was used since the mixability of the mixture in polysulfide aqueous solution is greater than either PEG-4000 alone or PEG-20000 alone. For simplicity, this mixture is simplified as PEG hereafter unless specially specified. The selection of CdSe with particle size of 5.4 ± 0.4 nm QD sensitizer is due to its facile and well-developed synthetic method and the relatively good photovoltaic performance high-reproducibility for resulting QDSCs.[41,46,49] All cell devices were constructed by assembling the sensitized photoanode, $Cu_{2-x}S$/FTO counter electrode and polysulfide electrolytes containing different concentrations of PEG as the hole transporter. Details about experiments are described in the Experimental section. To minimize the sampling deviation, the average photovoltaic performance of cell devices were obtained by measuring at least five parallel devices under AM 1.5G one sun illumination.

Photovoltaic performance

The dependence of photovoltaic performance of CdSe QDSCs on the concentration of PEG in polysulfide electrolyte is shown in Fig. 1. For clarity, the photovoltaic parameters of both average values and champion cells corresponding to cells devices based on various concentration of PEG additives in polysulfide electrolyte solution are summarized in Table 1. The *J*-*V* curves and photovoltaic parameters of each tested cell devices based on polysulfide electrolyte containing different concentrations of PEG additive are available in Fig. S3−S7 and Table S1−S5 of the ESI.† Experimental data shows that the PCEs of QDSCs are systematically improved with the increase of the PEG concentration in the polysulfide electrolyte. Since the up-limit of mixability of PEG with the adopted polysulfide electrolyte solution at room temperature is ~15%, investigation on higher PEG concentration has to be given up. Even though the PEG concentration is as low as 1 wt% in the polysulfide electrolyte, an enhancement of 3.3% in the PCE of the resultant cells is obtained in comparison with the reference cells in the absence of PEG in the electrolyte. The cells based on 15 wt% PEG in the polysulfide electrolyte possess the best PCE of 6.74% (short-circuit J_{sc} = 15.66 mA/cm^2, open-circuit voltage V_{oc} = 0.646 V, fill factor FF = 0.666) under AM 1.5G one sun illumination, with an improvement of 16.2% in PCE compared to the reference cells. It is highlighted that the obtained 6.74% PCE is believed to be one of the highest efficiencies in the CdSe based QDSCs.

The enhancement of PCE of QDSCs could be ascribed to the reduction of charge recombination between the photoanode and electrolyte solution *via* the steric hindrance effect of PEG absorbed on TiO_2/QDs/ interfaces.

From Fig. 1b, c, we can further find out that the improved PCE in the resulting cells is mainly derived from the enhanced V_{oc} and FF values, while the contribution from the J_{sc} can be negligible. The unchanged J_{sc} values corresponding to different electrolyte compositions is also supported by the similar incident-photon-to-current efficiency (IPCE) curves as showed in Fig. 1d. The similar IPCE properties indicate the similar electron collection and/or injection efficiency of different type of cells.

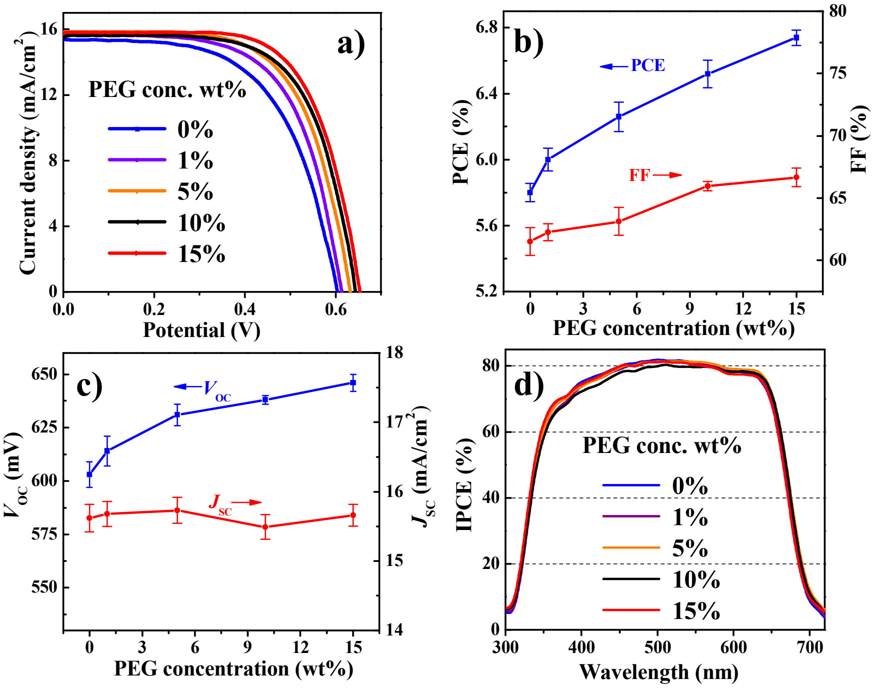

Fig. 1. (a) *J-V* curves of champion CdSe QDSCs based on polysulfide electrolyte containing different concentrations of PEG additive. The dependence of average photovoltaic performance on the concentration of PCE additive in polysulfide electrolyte: (b) dependence of PCE and FF, and (c) dependence of V_{oc} and J_{sc} on PEG concentration. (d) Typical incident photon to current efficiency (IPCE) curves.

Table 1. Main photovoltaic parameters for QDSCs based on polysulfide electrolyte containing different concentrations of PEG additives under the irradiation of AM 1.5G 100 mW/cm^{-2} intensity.

PEG Concentration (wt%)	J_{sc} (mA·cm^{-2})	V_{oc} (V)	FF (%)	PCE (%)[a]
0%	15.62(15.39)	0.603(0.604)	61.52(63.16)	5.80±0.055(5.87)
1%	15.68(15.72)	0.614(0.621)	62.26(62.49)	6.00±0.069(6.10)
5%	15.73(15.84)	0.631(0.639)	63.13(62.83)	6.26±0.089(6.36)
10%	15.49(15.63)	0.638(0.642)	65.96(66.28)	6.52±0.084(6.65)
15%	15.66(15.81)	0.646(0.643)	66.68(66.97)	6.74±0.046(6.81)

[a] average value with standard deviation based on 5 cell devices in parallel. The numbers in parentheses represent the values obtained for the champion cells.

Electrochemical impedance spectroscopy (EIS)

To unravel the mechanism of the enhanced V_{oc} and FF values in the resultant cell devices with introduction of PEG additives in the polysulfide electrolyte, electrochemical impedance spectra (EIS) measurements were employed for the cell devices containing different concentration of PEG in the polysulfide electrolyte in the dark condition under different forward bias, and the electrochemical parameters were extracted and analyzed with use of the standard models for QDSCs. Impedance characterization bears the capability to separate the effects of different parts in the sell device, which include sensitized photoanode, counter electrode, diffusion in the electrolyte, and series resistance at each applied forward bias (V_{app}). Fig. 2 shows the chemical capacitance (C_{μ}) and recombination resistance (R_{rec}) extracted from the corresponding Nyquist curves, and the detailed Nyquist curves for each cells at different forward bias are given in Fig. S8 of the ESI.† In IS spectra, it has been well established that C_{μ} reflects the dependence of electron density on the Fermi level, and therefore monitors the distribution of traps states in the band gap of the electron conductor (herein, TiO_2). R_{rec} is inversely proportional to the charge recombination rate in the interface between TiO_2/electrolyte. As shown in Fig. 2a, each cells exhibits similar C_{μ} values under each forward bias. This indicates that the PEG additive in polysulfide electrolyte does not affect the energy level of conduction band or the density of states of TiO_2. However, with the increase of the added PEG concentration in polysulfide electrolyte, the R_{rec} values are systematically enhanced in the whole applied forward bias range, as illustrated in Fig. 2b. For clarity, Nyquist plots of the cell devices based on polysulfide electrolyte containing various concentration of PEG additives at forward bias of −0.60 V, which is near to the V_{oc} value of the cells, are given in Fig. 2c, and the extracted EIS parameters are shown in Table 2. These results indicate that the recombination between TiO_2/QDs/electrolyte interfaces was effectively reduced by the PEG additive in polysulfide electrolyte.

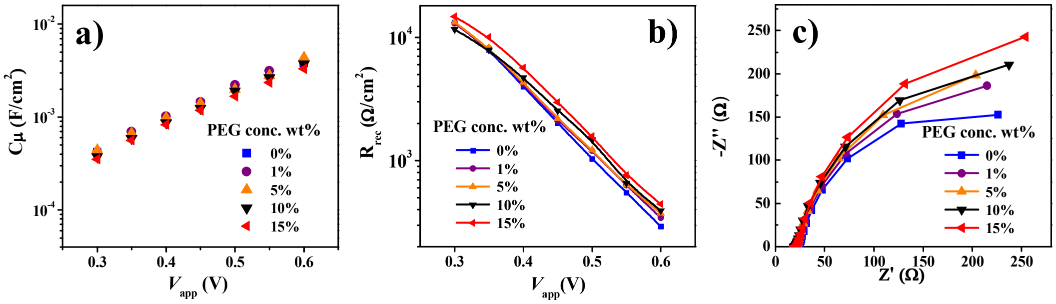

Fig. 2. Electrochemical impedance spectroscopy (EIS) characterization of QDSC based on polysulfide electrolyte containing different concentrations of PEG additives: a) chemical capacitance C_{μ}, b) recombination resistance R_{rec}, and c) Nyquist plots in dependence of the applied voltage V_{app} of each cells at −0.60 V forward bias.

Table 2. Simulated Values of Resistance (R) and Capacitance (C) under the Forward Bias of −0.6 V of the cell devices based on polysulfide electrolyte containing different concentrations of PEG additive.

PEG Concentration (wt%)	R_s (Ω·cm^2)	R_{CE} (Ω·cm^2)	R_{rec} (Ω·cm^2)	C_{μ} (mF·cm^{-2})
0%	19.8	4.89	292	37.8
1%	25.7	5.38	343	38.8
5%	24.2	6.61	373	43.7
10%	19.6	5.41	393	37.3
15%	22.8	4.16	445	33.1

Open circuit voltage decay (OCVD)

The effect of PEG on the performance of the cell devices was further evaluated by open circuit voltage decay (OCVD) measurement that was usually used to unveil the charge recombination processes.[50] Since the electrolyte containing 15% PEG corresponding to the best photovoltaic performance, henceforth we only compare the cell performance based on 15% PEG in polysulfide electrolyte with those based on convenient polysulfide electrolyte without the addition of PEG. In a typical measurement process, the studied cell was first irradiated to a steady state by a white LED of 100 mW/cm^2 and the V_{oc} decay information was then recorded after turning off the light. As can be seen from Fig. 3a, PEG-polysulfide electrolyte based cell exhibits higher V_{oc} and slower decay kinetics in comparison with that of the plain polysulfide electrolyte based cell, indicating the recombination rate of photo-generated electrons with the oxidized species in the electrolyte was significantly reduced with the existence of PEG additive in the electrolyte. The decrease of the electron recombination rate can also be revealed by the electron lifetime (τ_n), which was calculated from eq. 1 and the dependence of τ_n on potential is illustrated in Fig. 3b:

$$\tau_n = -\frac{k_B T}{e}\left(\frac{dV_{oc}}{dt}\right)^{-1} \qquad (1)$$

where, k_B is the Boltzmann constant, T is the absolute temperature, and e is the electronic charge.[51] From Fig. 3b, one can find that τ_n values of PEG-polysulfide electrolyte based cell are obviously longer than that of reference cell at the identical voltage, demonstrating that the photo-generated electrons lifetime are considerably increased by adding PEG in polysulfide electrolyte.

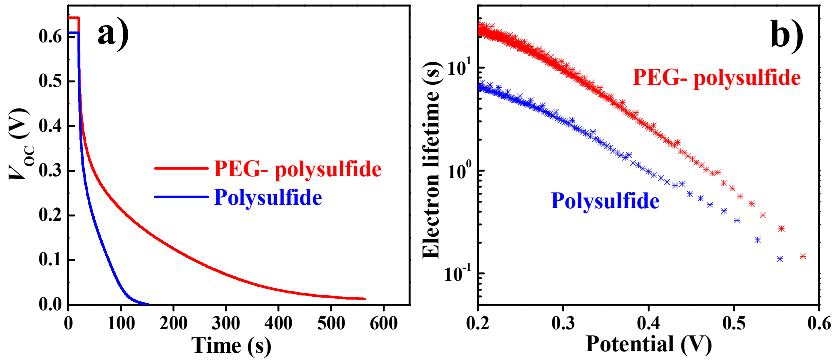

Fig. 3. Open circuit voltage decay (OCVD) measurement of QDSCs based on PEG-polysulfide electrolyte and the reference polysulfide electrolyte: a) the V_{oc} decay curves, b) the electron lifetime curves extracted from OCVD.

Cell stability

Long-term stability of photovoltaic performance is indispensable for the practical application of QDSCs,[9,33,52,53] but is often overlooked in most reports. The performance stability of the sealed cells based on polysulfide electrolyte containing 15 wt% PEG was compared with that of cells based on the conventional polysulfide electrolyte without the PEG additive under continuous irradiation condition by an AM 1.5 G solar simulator with intensity of 100 mW/cm^2 at room temperature. As shown in Fig. 4, the photovoltaic performance for both cells exhibits a rapid increase in the first 2 h. This phenomena is commonly observed in liquid-junction solar cells, which could be attributed to the capillary effect of electrolyte permeation into the mesoporous TiO_2 film. As anticipated, the cells based on polysulfide electrolyte with the existence of PEG show better stability than those in the absence of PEG additives. Experimental results demonstrate that the normalized PCE values for the reference cells start to decline gradually after 12 h, and reach to about 82% of the initial values in the course of 20 h irradiation; while the cells based on electrolyte containing PEG additive keeps nearly the best performance in the course of 30 h irradiation, and the performance decline started at ~35 h irradiation. The temporal evolution of *J-V* curves for cell devices based on the conventional polysulfide electrolyte and the PEG-polysulfide electrolyte are available in Fig. S9 of the ESI.† The improved stability could be stemmed from the PEG layer adsorbed on QD surface, which prevents photo-corrosion reported in chalcogenides under polysulfide and illumination conditions.[9]

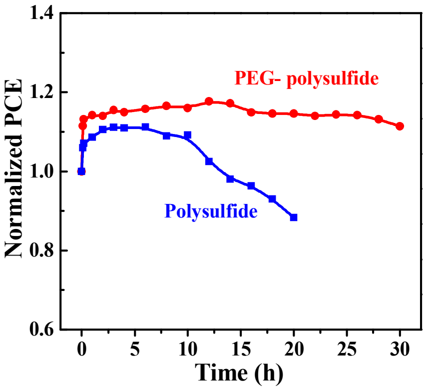

Fig. 4. Temporal evolution of PCE of CdSe QDSCs based on polysulfide electrolyte with or without the presence of PEG additive under the continuous irradiation by an AM 1.5 G solar simulator with intensity of 100 mW/cm^2 at room temperature.

4. Conclusions

In summary, an unprecedented PCE of 6.74% for CdSe-sensitized QDSCs was obtained by using the modified polysulfide electrolyte with PEG as additives. In comparison with that of CdSe-sensitized QDSC based on typical polysulfide electrolyte, the PCE of cells using PEG-polysulfide electrolyte was significant improved, and long-term stability (30 h under illumination) was also obtained. The higher PCE of the PEG-polysulfide electrolyte based cells is mainly benefited from the enhancement of V_{oc} and FF, which could be attributed to the reduction of the charge recombination between TiO_2/QDs/electrolyte interfaces. The reduction of charge recombination was confirmed by EIS and OCVD.

Acknowledgements

We acknowledge the National Natural Science Foundation of China (No. 21421004, 91433106, 21175043, and 21301059), the Science and Technology Commission of Shanghai Municipality (11JC1403100 and 12NM0504101), the Fundamental Research Funds for the Central Universities in China for financial support.

† Electronic supplementary information (ESI) available: Optical properties and the TEM image of the oil-soluble CdSe QDs. Absorption spectra of the CdSe QDs films before and after with polysulfide electrolyte with and without 15 wt% PEG additives treatment. *J-V* curves and photovoltaic parameters of each tested cell devices based on polysulfide electrolyte containing different concentrations of PEG additive. Temporal evolution of *J-V* curves for QDSCs based on polysulfide electrolyte and PEG-polysulfide electrolyte under continuous irradiation. Nyquist curves for polysulfide electrolyte and PEG-polysulfide electrolyte based cells at different forward bias. Detailed procedures for preparation of the copper sulfide counter electrode.

References

1 I. J. Kramer and E. H. Sargent, *Chem. Rev.*, 2014, **114**, 863−882.

2 O. E. Semonin, J. M. Luther, S. Choi, H.-Y. Chen, J. Gao, A. J. Nozik and M. C. Beard, *Science*, 2011, **334**, 1530−1533.

3 E. H. Sargent, *Nat. Photon*., 2012, **6**, 133−135.

4 P. V. Kamat, K. Tvrdy, D. R. Baker and J. G. Radich, *Chem. Rev.*, 2010, **110**, 6664−6688.

5 J. R. Swierk and T. E. Mallouk, *Chem. Soc. Rev.*, 2013, **42**, 2357−2387.

6 B. Oregan and M. Grätzel, *Nature*, 1991, **353**, 737–740.

7 S. Mathew, A. Yella, P. Gao, R. Humphry-Baker, B. F. E. Curchod, N. Ashari-Astani, I. Tavernelli, U. Rothlisberger, M. K. Nazeeruddin and M. Grätzel, *Nat. Chem.*, 2014, **6**, 242–247.

8 P. V. Kamat, J. A. Christians and J. G. Radich, *Langmuir*, 2014, **30**, 5716−5725.

9 V. Chakrapani, D. Baker and P. V. Kamat, *J. Am. Chem. Soc.*, 2011, **133**, 9607–9615.

10 H. Zhu, N. Song and T. Lian, *J. Am. Chem. Soc.*, 2013, **135**, 11461–11464.

11 G. Hodes, J. Manassen and D. Cahen, *J. Electrochem. Soc.*, 1980, **127**, 544–549.

12 Y. -L. Lee and C. -H. Chang, *J. Power Sources*, 2008, **185**, 584–588.

13 Z. Pan, I. Mora-Seró, Q. Shen, H. Zhang, Y. Li, K. Zhao, J. Wang, X. Zhong and J. Bisquert, *J. Am. Chem. Soc.*, 2014, **136**, 9203−9210.

14 J. Wang, I. Mora-Seró, Z. Pan, K. Zhao, H. Zhang, Y. Feng, G. Yang, X. Zhong and J. Bisquert, *J. Am. Chem. Soc.*, 2013, **135**, 15913−15922.

15 S. Jiao, Q. Shen, I. Mora-Seró, J. Wang, Z. Pan, K. Zhao, Y. Kuga, X. Zhong, J. Bisquert, *ACS Nano*, 2015, **9**, 908–915.

16 A. V. Akimov, A. J. Neukirch and O. V. Prezhdo, *Chem. Rev.*, 2013, **113**, 4496−4565.

17 Z. Ning, Y. Fu and H. Tian, *Energy Environ. Sci.*, 2010, **3**, 1170–1181.

18 G. J. Hodes, *J. Phys. Chem. C*, 2008, **112**, 17778–17787.

19 A. Hagfeldt, G. Boschloo, L. Sun, L. Kloo and H. Pettersson, *Chem. Rev.*, 2010, **110**, 6595–6663.

20 I. Mora-Seró and J. Bisquert, *Nano Lett.*, 2003, **3**, 945−949.

21 C. -H. Chang and Y. -L. Lee, *Appl. Phys. Lett.*, 2007, **91**,053503.

22 H. Lee, M. Wang, P. Chen, D. R. Gamelin, S. M. Zakeeruddin, M. Grätzel and M. K. Nazeeruddin, *Nano Lett.*, 2009, **9**, 4221–4227.

23 S. Y. Chae, Y. J. Hwang, O. -S. Joo, *RSC Adv.*, 2014, **4**, 26907–26911.

24 Z. Ning, C. Yuan, H. Tian, Y. Fu, L. Li, L. Sun and H. Agren, *J. Mater. Chem.*, 2012, **22**, 6032−6037.

25 L. Li, X. Yang, J. Gao, H. Tian, J. Zhao, A. Hagfeldt and L. Sun, *J. Am. Chem. Soc.*, 2011, **133**, 8458–8460.

26 T. Shu, X. Li, Z. Ku, S. Wang, S. Wu, X. Jin and C. Hu, *Electrochim. Acta*, 2014, **137**, 700–704.

27 I. Mora-Seró, S. Giménez, F. Fabregat-Santiago, R. Gómez, Q. Shen, T. Toyoda and J. Bisquert, *Acc. Chem. Res.*, 2009, **42**, 1848–1857.

28 K. Hara, Y. Dan-oh, C. Kasada, Y. Ohga, A. Shinpo, S. Suga, K. Sayama and H. Arakawa, *Langmuir*, 2004, **20**, 4205−4210.

29 G. Boschloo, L. Häggman and A. Hagfeldt, *J. Phys. Chem. B*, 2006*,* **110***,* 13144–13150.

30 C. Zhang, Y. Huang, Z. Huo, S. Chen and S. Dai, *J. Phys. Chem. C*, 2009, **113**, 21779–21783.

31 Z. Yu, Q. Zhang, D. Qin, Y. Luo, D. Li, Q. Shen, T. Toyoda and Q. Meng, *Electrochem. Commun*., 2010, **12**, 1776–1779.

32 H. Chen, L. Lin, X. Yu, K. Qiu, X. Lü, D. Kuang and C. Su, *Electrochim. Acta*, 2013, **92***,* 117–123.

33 V. Jovanovski, V. González-Pedro, S. Giménez, E. Azaceta, G. Cabañero, H. Grande, R. Tena-Zaera, I. Mora-Seró and J. Bisquert, *J. Am. Chem. Soc.*, 2011, **133**, 20156–20159.

34 M. C. Sekhar, K. Santhosh, J. P. Kumar, N. Mondal, S. Soumya and A. Samanta, *J. Phys. Chem. C*, 2014, **118**, 18481−18487.

35 S. Wang, Q. Zhang, Y. Xu, D. Li, Y. Luo and Q. Meng, *J. Power Sources*, 2013, **224**, 152–157.

36 H. Kim, I. Hwang and K. Yong, *Appl. Mater. Interfaces*, 2014, **6**, 11245−11253.

37 M. Shalom, S. Rühle, I. Hod, S. Yahav and A. Zaban, *J. Am. Chem. Soc.*, 2009, **131**, 9876–9877.

38 E. M. Barea, M. Shalom, S. Giménez, I. Hod, I. Mora-Seró, A. Zaban and J. Bisquert, *J. Am. Chem. Soc.*, 2010, **132**, 6834–6839.

39 S. Laurent, D. Forge, M. Port, A. Roch, C. Robic, L. V. Elst and R. N. Muller, *Chem. Rev.*, 2008, **108**, 2064–2110.

40 T. Reihs, M. Muller, K. Lunkwitz, *Colloids Surface A*, 2003, 212, 79–95.

41 X. Zhong, Y. Feng and Y. Zhang, *J. Phys. Chem. C*, 2007, **111**, 526–531.

42 H. Zhang, K. Cheng, Y. Hou, Z. Fang, Z. Pan, W. Wu, J. Hua and X. Zhong, *Chem. Commun*., 2012, **48**, 11235−11237.

43 W. Li and X. Zhong, *J. Phys. Chem. Lett.*, 2015, **6**, 796−806.

44 Z. Du, H. Zhang, H. Bao and X. Zhong, *J. Mater. Chem. A*, 2014, **2**, 13033–13040.

45 K. Zhao, Z. Pan, I. Mora-Seró, E. Canovas, H. Wang, Y. Song, X. Gong, J. Wang, M. Bonn, J. Bisquert and X. Zhong, *J. Am. Chem. Soc.*, 2015, **137**, 5602–5609.

46 H, Zhang, H, Bao and X. Zhong, *J. Mater. Chem. A*, 2015, **3**, 6557−6564.

47 J. Yang, T. Oshima, W. Yindeesuk, Z. Pan, X. Zhong and Q. Shen, *J. Mater. Chem. A*, 2014, **2**, 20882–20888.

48 S. Yang, X. Zhou, J. Zhang and Z. Liu, *J. Mater. Chem.*, 2010, **20**, 8086–8091.

49 J. Tian, L. Lv, C. Fei, Y. Wang, X. Liua and G. Cao, *J. Mater. Chem. A*, 2014, **2**, 19653−19659.

50 J. Bisquert, A. Zaban, M. Greenshtein and I. Mora-Seró, *J. Am. Chem. Soc.*, 2004, **126**, 13550–13559.

51 V. González-Pedro, X. Xu, I. Mora-Seró and J. Bisquert, *ACS Nano*, 2010, **4**, 5783–5790.

52 K. Zhao, H. Yu, H. Zhang and X. Zhong, *J. Phys. Chem. C*, 2014, **118**, 5683−5690.

53 Y. Yang, L. Zhu, H. Sun, X. Huang, Y. Luo, D. Li and Q. Meng, *ACS Appl. Mater. Interfaces*, 2012, **4**, 6162–6168.

Table of Contents (TOC)

Performance enhancement of quantum dot sensitized solar cells by adding electrolyte additives

Jun Du, Xinxin Meng, Ke Zhao, Yan Li* and Xinhua Zhong*